

# Generalized Min-Max Kernel and Generalized Consistent Weighted Sampling

Ping Li

Department of Statistics and Biostatistics  
 Department of Computer Science  
 Rutgers University  
 Piscataway, NJ 08854, USA  
 pingli@stat.rutgers.edu

## Abstract

We propose the “generalized min-max” (GMM) kernel as a measure of data similarity, where data vectors can have both positive and negative entries. GMM is positive definite as there is an associate hashing method named “generalized consistent weighted sampling” (GCWS) which linearizes this (nonlinear) kernel. A natural competitor of GMM is the radial basis function (RBF) kernel, whose corresponding hashing method is known as the “random Fourier features” (RFF). An extensive experimental study on classifications of **50** publicly available datasets demonstrates that both the GMM and RBF kernels can often substantially improve over linear classifiers. Furthermore, the GCWS hashing method typically requires substantially fewer samples than (the normalized) RFF in order to achieve similar classification accuracies.

To understand the property of random Fourier features (RFF), we derive the theoretical variances of RFF and its normalized version (which we name as NRFF). Overall, the relative (to the expectation) variances of RFF and NRFF are substantially larger than the relative variance of GCWS. This helps explain the superb empirical results of GCWS compared to RFF (NRFF).

Additional comparisons are available in public domains, although most of them are not formally published. For example, see [17] for comparisons with “sign stable random projections” which provide hashing methods for a series of nonlinear kernels. See [15] for the work on linearizing GMM with the Nystrom method. See [19] for theoretical analysis of the GMM kernel as well as the cosine kernel. Also, see [14] for comparisons with the histogram intersection kernel.

We expect that GMM and GCWS will be adopted in practice for large-scale statistical machine learning applications and efficient near neighbor search (as GMM generates discrete hash values).

## 1 Introduction

It is popular in machine learning practice to use linear algorithms such as logistic regression or linear SVM. It is also known that one can often improve the performance of linear methods by using nonlinear algorithms such as kernel SVMs, if the computational/storage burden can be resolved. The purpose of this paper is to introduce an effective measure of data similarity termed “generalized min-max” (GMM) kernel and the associated hashing method named “generalized consistent weighted sampling” (GCWS), which efficiently converts this nonlinear kernel into linear kernel.

We start the introduction with the basic linear kernel. Consider two data vectors  $u, v \in \mathbb{R}^D$ . It is common to use the normalized linear kernel (i.e., the correlation):

$$\rho = \rho(u, v) = \frac{\sum_{i=1}^D u_i v_i}{\sqrt{\sum_{i=1}^D u_i^2} \sqrt{\sum_{i=1}^D v_i^2}} \quad (1)$$

This normalization step is in general a recommended practice. For example, when using LIBLINEAR or LIBSVM packages [6], it is often suggested to first normalize the input data vectors to unit  $l_2$  norm. In addition to packages such as LIBLINEAR which implement batch linear algorithms, methods based on stochastic gradient descent (SGD) become increasingly important especially for truly large industrial applications [2].

In this paper, the proposed GMM kernel is defined on general data types which can have both negative and positive entries. The basic idea is to first transform the original data into nonnegative data and then compute the min-max kernel [20, 10, 14] on the transformed data.

### 1.1 Data Transformation

Consider the original data vector  $u_i$ ,  $i = 1$  to  $D$ . We define the following transformation, depending on whether an entry  $u_i$  is positive or negative:<sup>1</sup>

$$\begin{cases} \tilde{u}_{2i-1} = u_i, & \tilde{u}_{2i} = 0 & \text{if } u_i > 0 \\ \tilde{u}_{2i-1} = 0, & \tilde{u}_{2i} = -u_i & \text{if } u_i \leq 0 \end{cases} \quad (2)$$

For example, when  $D = 2$  and  $u = [-5 \ 3]$ , the transformed data vector becomes  $\tilde{u} = [0 \ 5 \ 3 \ 0]$ .

### 1.2 Generalized Min-Max (GMM) Kernel

Given two data vectors  $u, v \in \mathbb{R}^D$ , we first transform them into  $\tilde{u}, \tilde{v} \in \mathbb{R}^{2D}$  according to (2). Then the generalized min-max (GMM) similarity is defined as

$$GMM(u, v) = \frac{\sum_{i=1}^{2D} \min(\tilde{u}_i, \tilde{v}_i)}{\sum_{i=1}^{2D} \max(\tilde{u}_i, \tilde{v}_i)} \quad (3)$$

We will show in Section 3 that GMM is indeed an effective measure of data similarity through an extensive experimental study on kernel SVM classification.

It is generally nontrivial to scale nonlinear kernels for large data [3]. In a sense, it is not practically meaningful to discuss nonlinear kernels without knowing how to compute them efficiently (e.g., via hashing). In this paper, we focus on the generalized consistent weighted sampling (GCWS).

### 1.3 Generalized Consistent Weighted Sampling (GCWS)

Algorithm 1 summarizes the “generalized consistent weighted sampling” (GCWS). Given two data vectors  $u$  and  $v$ , we transform them into nonnegative vectors  $\tilde{u}$  and  $\tilde{v}$  as in (2). We then apply the original “consistent weighted sampling” (CWS) [20, 10] to generate random tuples:

$$(i_{\tilde{u},j}^*, t_{\tilde{u},j}^*) \quad \text{and} \quad (i_{\tilde{v},j}^*, t_{\tilde{v},j}^*), \quad j = 1, 2, \dots, k \quad (4)$$

where  $i^* \in [1, 2D]$  and  $t^*$  is unbounded. Following [20, 10], we have the basic probability result.

---

<sup>1</sup> This transformation can be generalized by considering a “center vector”  $\mu_i$ ,  $i = 1$  to  $D$ , such that

$$\begin{cases} \tilde{u}_{2i-1} = u_i - \mu_i, & \tilde{u}_{2i} = 0 & \text{if } u_i > \mu_i \\ \tilde{u}_{2i-1} = 0, & \tilde{u}_{2i} = -u_i + \mu_i & \text{if } u_i \leq \mu_i \end{cases}$$

In this paper, we always use  $\mu_i = 0$ ,  $\forall i$ . Note that the same center vector  $\mu$  should be used for all data vectors.

## Theorem 1

$$\Pr \{(i_{\tilde{u},j}^*, t_{\tilde{u},j}^*) = (i_{\tilde{v},j}^*, t_{\tilde{v},j}^*)\} = GMM(u, v) \quad (5)$$

---

### Algorithm 1 Generalized Consistent Weighted Sampling (GCWS)

---

**Input:** Data vector  $u = (i = 1 \text{ to } D)$

**Transform:** Generate vector  $\tilde{u}$  in  $2D$ -dim by (2)

**Output:** Consistent uniform sample  $(i^*, t^*)$

---

For  $i$  from 1 to  $2D$

$r_i \sim \text{Gamma}(2, 1)$ ,  $c_i \sim \text{Gamma}(2, 1)$ ,  $\beta_i \sim \text{Uniform}(0, 1)$

$t_i \leftarrow \lfloor \frac{\log \tilde{u}_i}{r_i} + \beta_i \rfloor$ ,  $z_i \leftarrow \exp(r_i(t_i - \beta_i))$ ,  $a_i \leftarrow c_i / (z_i \exp(r_i))$

End For

$i^* \leftarrow \arg \min_i a_i$ ,  $t^* \leftarrow t_{i^*}$

---

With  $k$  samples, we can simply use the averaged indicator to estimate  $GMM(u, v)$ . By property of the binomial distribution, we know the expectation ( $E$ ) and variance ( $Var$ ) are

$$E [1\{i_{\tilde{u},j}^* = i_{\tilde{v},j}^* \text{ and } t_{\tilde{u},j}^* = t_{\tilde{v},j}^*\}] = GMM(u, v), \quad (6)$$

$$Var [1\{i_{\tilde{u},j}^* = i_{\tilde{v},j}^* \text{ and } t_{\tilde{u},j}^* = t_{\tilde{v},j}^*\}] = (1 - GMM(u, v))GMM(u, v) \quad (7)$$

The estimation variance, given  $k$  samples, will be  $\frac{1}{k}(1 - GMM)GMM$ , which vanishes as GMM approaches 0 or 1, or as the sample size  $k \rightarrow \infty$ .

## 1.4 0-bit GCWS for Linearizing GMM Kernel SVM

The so-called “0-bit” GCWS idea is that, based on intensive empirical observations [14], one can safely ignore  $t^*$  (which is unbounded) and simply use

$$\Pr \{i_{\tilde{u},j}^* = i_{\tilde{v},j}^*\} \approx GMM(u, v) \quad (8)$$

For each data vector  $u$ , we obtain  $k$  random samples  $i_{\tilde{u},j}^*$ ,  $j = 1$  to  $k$ . We store only the lowest  $b$  bits of  $i^*$ , based on the idea of [18]. We need to view those  $k$  integers as locations (of the nonzeros) instead of numerical values. For example, when  $b = 2$ , we should view  $i^*$  as a vector of length  $2^b = 4$ . If  $i^* = 3$ , then we code it as  $[1 \ 0 \ 0 \ 0]$ ; if  $i^* = 0$ , we code it as  $[0 \ 0 \ 0 \ 1]$ . We can concatenate all  $k$  such vectors into a binary vector of length  $2^b \times k$ , with exactly  $k$  1’s.

Note that for linear methods, the computational cost is largely determined by the number of nonzeros in each data vector, i.e.,  $k$  in our case. We recommend to use a fairly large  $b$  if possible, for example,  $b = 4$  or  $8$ . In our experiments, we can see that even  $b = 4$  can usually achieve good results.

The natural competitor of the GMM kernel is the RBF (radial basis function) kernel, and the competitor of the GCWS hashing method is the RFF (random Fourier feature) algorithm.

## 2 RBF Kernel and Random Fourier Features (RFF)

The radial basis function (RBF) kernel is widely used in machine learning and beyond. In this study, for convenience (e.g., parameter tuning), we recommend the following version:

$$RBF(u, v; \gamma) = e^{-\gamma(1-\rho)} \quad (9)$$

where  $\rho = \rho(u, v)$  is the correlation defined in (1) and  $\gamma > 0$  is a crucial tuning parameter. Based on Bochners Theorem [24], it is known [22] that, if we sample  $w \sim \text{uniform}(0, 2\pi)$ ,  $r_i \sim N(0, 1)$  i.i.d., and let  $x = \sum_{i=1}^D u_i r_{ij}$ ,  $y = \sum_{i=1}^D v_i r_{ij}$ , where  $\|u\|_2 = \|v\|_2 = 1$ , then we have

$$E \left( \sqrt{2} \cos(\sqrt{\gamma}x + w) \sqrt{2} \cos(\sqrt{\gamma}y + w) \right) = e^{-\gamma(1-\rho)} \quad (10)$$

This provides a nice mechanism for linearizing the RBF kernel and the RFF method has become very popular in machine learning, computer vision, and beyond, e.g., [21, 27, 1, 8, 5, 28, 9, 25, 4, 23].

It turns out that, for nonnegative data, one can simplify (10) by removing the random variable  $w$ , based on the following interesting result:

$$E(\cos(\sqrt{\gamma}x) \cos(\sqrt{\gamma}y)) = \frac{1}{2}e^{-\gamma(1-\rho)} + \frac{1}{2}e^{-\gamma(1+\rho)} = fRBF(u, v; \gamma) \quad (11)$$

which is monotonic when  $\rho \geq 0$ . Later in the paper we will also report the performance of fRBF (“folded RBF”) kernel and its hashing method on a large collection of nonnegative datasets.

**Theorem 2** *Given  $x \sim N(0, 1)$ ,  $y \sim N(0, 1)$ ,  $E(xy) = \rho$ , and  $w \sim \text{uniform}(0, 2\pi)$ , we have*

$$E \left[ \sqrt{2} \cos(\sqrt{\gamma}x + w) \sqrt{2} \cos(\sqrt{\gamma}y + w) \right] = e^{-\gamma(1-\rho)} \quad (12)$$

$$E[\cos(\sqrt{\gamma}x) \cos(\sqrt{\gamma}y)] = \frac{1}{2}e^{-\gamma(1-\rho)} + \frac{1}{2}e^{-\gamma(1+\rho)} \quad (13)$$

$$\text{Var} \left[ \sqrt{2} \cos(\sqrt{\gamma}x + w) \sqrt{2} \cos(\sqrt{\gamma}y + w) \right] = \frac{1}{2} + \frac{1}{2} \left( 1 - e^{-2\gamma(1-\rho)} \right)^2 \quad (14)$$

The proof for the variance (14) can also be found in [26]. One can immediately see that the variance of RFF might be too large. On the other hand, when we train an SVM classifier, we often first normalize the input feature vector to have unit  $l_2$  norm. Hence, we really should analyze the variance of “normalized RFF (NRFF)”. The results are presented in Theorem 3.

**Theorem 3** *Consider  $k$  iid samples  $(x_j, y_j, w_j)$  where  $x_j \sim N(0, 1)$ ,  $y_j \sim N(0, 1)$ ,  $E(x_j y_j) = \rho$ ,  $w_j \sim \text{uniform}(0, 2\pi)$ ,  $j = 1, 2, \dots, k$ . Let  $X_j = \sqrt{2} \cos(\sqrt{\gamma}x_j + w_j)$  and  $Y_j = \sqrt{2} \cos(\sqrt{\gamma}y_j + w_j)$ . As  $k \rightarrow \infty$ , the following asymptotic normality holds:*

$$\sqrt{k} \left( \frac{\sum_{j=1}^k X_j Y_j}{\sqrt{\sum_{j=1}^k X_j^2} \sqrt{\sum_{j=1}^k Y_j^2}} - e^{-\gamma(1-\rho)} \right) \xrightarrow{D} N(0, V_{n,\rho,\gamma}) \quad (15)$$

where

$$V_{n,\rho,\gamma} = V_{\rho,\gamma} - \frac{1}{4}e^{-2\gamma(1-\rho)} \left[ 3 - e^{-4\gamma(1-\rho)} \right] \quad (16)$$

$$V_{\rho,\gamma} = \frac{1}{2} + \frac{1}{2} \left( 1 - e^{-2\gamma(1-\rho)} \right)^2 \quad (17)$$

Obviously,  $V_{n,\rho,\gamma} < V_{\rho,\gamma}$  (in particular,  $V_{n,\rho,\gamma} = 0$  at  $\rho = 1$ ), i.e., the variance of the normalized RFF is smaller than that of the original RFF. Figure 1 plots  $\frac{V_{n,\rho,\gamma}}{V_{\rho,\gamma}}$  to visualize the improvement.

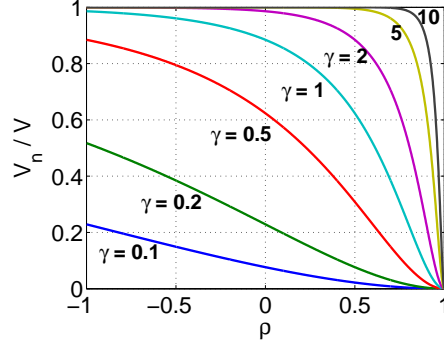


Figure 1: The ratio  $\frac{V_{n,\rho,\gamma}}{V_{\rho,\gamma}}$  from Theorem 3 for visualizing the improvement due to normalization.

Note that the theoretical results in Theorem 3 are asymptotic (i.e., for larger  $k$ ). With  $k$  samples, the variance of the original RFF is exactly  $\frac{V_{\rho,\gamma}}{k}$ , however the variance of the normalized RFF (NRFF) is written as  $\frac{V_{n,\rho,\gamma}}{k} + O\left(\frac{1}{k^2}\right)$ . It is important to understand the behavior when  $k$  is not large. For this purpose, Figure 2 presents the simulated mean square error (MSE) results for estimating the RBF kernel  $e^{-\gamma(1-\rho)}$ , confirming that a): the improvement due to normalization can be substantial, and b): the asymptotic variance formula (16) becomes accurate for merely  $k > 10$ .

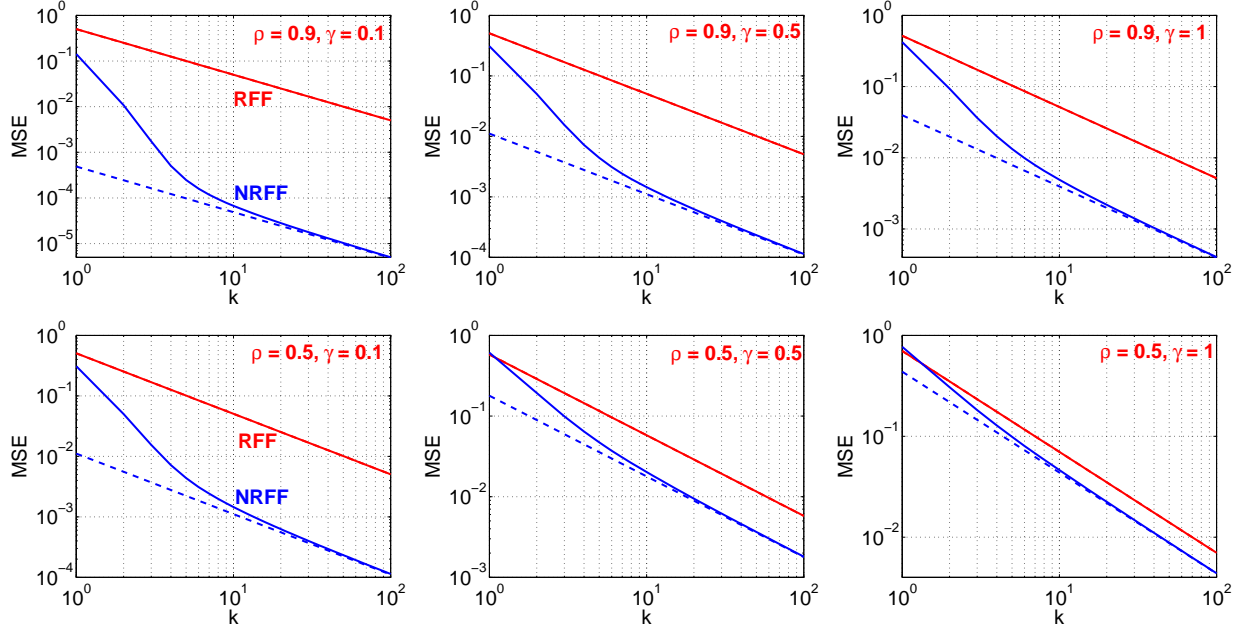


Figure 2: A simulation study to verify the asymptotic theoretical results in Theorem 3. With  $k$  samples, we estimate the RBF kernel  $e^{-\gamma(1-\rho)}$ , using both the original RFF and the normalized RFF (NRFF). With  $10^5$  repetitions at each  $k$ , we can compute the empirical mean square error:  $\text{MSE} = \text{Bias}^2 + \text{Var}$ . Each panel presents the MSEs (solid curves) for a particular choice of  $(\rho, \gamma)$ , along with the theoretical variances:  $\frac{V_{\rho,\gamma}}{k}$  and  $\frac{V_{n,\rho,\gamma}}{k}$  (dashed curves). The variance of the original RFF (curves above, or red if color is available) can be substantially larger than the MSE of the normalized RFF (curves below, or blue). When  $k > 10$ , the normalized RFF provides an unbiased estimate of the RBF kernel and its empirical MSE matches the theoretical asymptotic variance.

Next, we attempt to compare RFF with GCWS. While ultimately we can rely on classification accuracy as a metric for performance, here we compare their variances ( $Var$ ) relative to their expectations ( $E$ ) in terms of  $Var/E^2$ , as shown in Figure 3. For GCWS, we know  $Var/E^2 = E(1 - E)/E^2 = (1 - E)/E$ . For the original RFF, we have  $Var/E^2 = \left[ \frac{1}{2} + \frac{1}{2} (1 - E^2) \right] / E^2$ , etc.

Figure 3 shows that the relative variance of GCWS is substantially smaller than that of the original RFF and the normalized RFF, especially when  $E$  is not large. For the very high similarity region (i.e.,  $E \rightarrow 1$ ), both the normalized RFF and GCWS have substantially smaller relative variances than the original RFF.

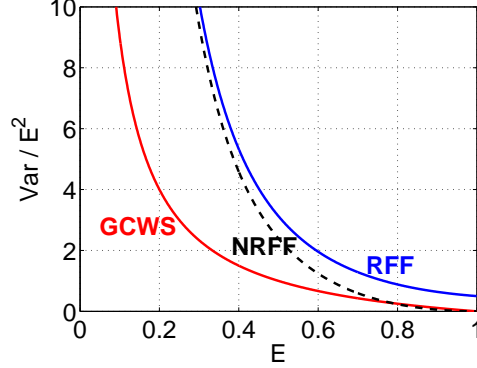


Figure 3: Ratio of the variance over the expectation square, denoted as  $Var/E^2$ , for the convenience of comparing RFF (and normalized RFF) with GCWS.

The results from Figure 3 provide an explanation why later we will observe that, in the classification experiments, GCWS typically needs substantially fewer samples than the normalized RFF, in order to achieve similar classification accuracies. Note that for practical data, the similarities among most data points are usually small (i.e., small  $E$ ) and hence it is not surprising that GCWS may perform substantially better.

In a sense, this drawback of RFF is expected, due to the nature of random projection method. For example, as shown in [16], the linear estimator of the correlation  $\rho$  using random projections has variance  $\frac{1+\rho^2}{k}$ , where  $k$  is the number of projections. In order to make the variance small, one will have to use many projections (i.e., large  $k$ ).

**Proof of Theorem 2:** The following three integrals will be useful in our proof:

$$\int_{-\infty}^{\infty} \cos(cx) e^{-x^2/2} dx = \sqrt{2\pi} e^{-c^2/2}$$

$$\begin{aligned} \int_{-\infty}^{\infty} \cos(c_1 x) \cos(c_2 x) e^{-x^2/2} dx &= \frac{1}{2} \int_{-\infty}^{\infty} [\cos((c_1 + c_2)x) + \cos((c_1 - c_2)x)] e^{-x^2/2} dx \\ &= \frac{\sqrt{2\pi}}{2} [e^{-(c_1+c_2)^2/2} + e^{-(c_1-c_2)^2/2}] \end{aligned}$$

$$\int_{-\infty}^{\infty} \sin(c_1 x) \sin(c_2 x) e^{-x^2/2} dx = \frac{\sqrt{2\pi}}{2} [e^{-(c_1-c_2)^2/2} - e^{-(c_1+c_2)^2/2}]$$

Firstly, we consider integers  $b_1, b_2 = 1, 2, 3, \dots$ , and evaluate the following general integral:

$$\begin{aligned}
& E(\cos(c_1x + b_1w) \cos(c_2y + b_2w)) \\
&= \frac{1}{2\pi} \int_0^{2\pi} E(\cos(c_1x + b_1t) \cos(c_2y + b_2t)) dt \\
&= \frac{1}{2\pi} \int_0^{2\pi} \int_{-\infty}^{\infty} \int_{-\infty}^{\infty} (\cos(c_1x + b_1t) \cos(c_2y + b_2t)) \frac{1}{2\pi} \frac{1}{\sqrt{1-\rho^2}} e^{-\frac{x^2+y^2-2\rho xy}{2(1-\rho^2)}} dx dy dt \\
&= \frac{1}{2\pi} \int_0^{2\pi} \int_{-\infty}^{\infty} \int_{-\infty}^{\infty} (\cos(c_1x + b_1t) \cos(c_2y + b_2t)) \frac{1}{2\pi} \frac{1}{\sqrt{1-\rho^2}} e^{-\frac{x^2+y^2-2\rho xy+\rho^2x^2-\rho^2y^2}{2(1-\rho^2)}} dx dy dt \\
&= \frac{1}{2\pi} \int_0^{2\pi} \int_{-\infty}^{\infty} \frac{1}{2\pi} \frac{1}{\sqrt{1-\rho^2}} e^{-\frac{x^2}{2}} \cos(c_1x + b_1t) dx \int_{-\infty}^{\infty} \cos(c_2y + b_2t) e^{-\frac{(y-\rho x)^2}{2(1-\rho^2)}} dy dt \\
&= \frac{1}{2\pi} \int_0^{2\pi} \int_{-\infty}^{\infty} \frac{1}{2\pi} e^{-\frac{x^2}{2}} \cos(c_1x + b_1t) dx \int_{-\infty}^{\infty} \cos(c_2y \sqrt{1-\rho^2} + c_2\rho x + b_2t) e^{-y^2/2} dy dt \\
&= \frac{1}{2\pi} \int_0^{2\pi} \int_{-\infty}^{\infty} \frac{1}{2\pi} e^{-\frac{x^2}{2}} \cos(c_1x + b_1t) \cos(c_2\rho x + b_2t) dx \int_{-\infty}^{\infty} \cos(c_2y \sqrt{1-\rho^2}) e^{-y^2/2} dy dt \\
&= \frac{1}{2\pi} \int_0^{2\pi} \int_{-\infty}^{\infty} \frac{1}{2\pi} e^{-\frac{x^2}{2}} \cos(c_1x + b_1t) \cos(c_2\rho x + b_2t) \sqrt{2\pi} e^{-\frac{c_2^2(1-\rho^2)}{2}} dx dt \\
&= \frac{1}{2\pi} \frac{1}{\sqrt{2\pi}} e^{-\frac{c_2^2(1-\rho^2)}{2}} \int_0^{2\pi} \int_{-\infty}^{\infty} e^{-\frac{x^2}{2}} \cos(c_1x + b_1t) \cos(c_2\rho x + b_2t) dx dt
\end{aligned}$$

Note that

$$\begin{aligned}
& \int_0^{2\pi} \cos(c_1x + b_1t) \cos(c_2\rho x + b_2t) dt \\
&= \int_0^{2\pi} \cos(c_1x) \cos(b_1t) \cos(c_2\rho x) \cos(b_2t) dt + \int_0^{2\pi} \sin(c_1x) \sin(b_1t) \sin(c_2\rho x) \sin(b_2t) dt \\
&\quad - \int_0^{2\pi} \cos(c_1x) \cos(b_1t) \sin(c_2\rho x) \sin(b_2t) dt - \int_0^{2\pi} \sin(c_1x) \sin(b_1t) \cos(c_2\rho x) \cos(b_2t) dt
\end{aligned}$$

When  $b_1 \neq b_2$ , we have

$$\begin{aligned}
\int_0^{2\pi} \cos(b_1t) \cos(b_2t) dt &= \frac{1}{2} \int_0^{2\pi} \cos(b_1t - b_2t) + \cos(b_1t + b_2t) dt = 0 \\
\int_0^{2\pi} \sin(b_1t) \sin(b_2t) dt &= \frac{1}{2} \int_0^{2\pi} \cos(b_1t - b_2t) - \cos(b_1t + b_2t) dt = 0
\end{aligned}$$

If  $b_1 = b_2$ , then

$$\int_0^{2\pi} \cos(b_1t) \cos(b_2t) dt = \int_0^{2\pi} \sin(b_1t) \sin(b_2t) dt = \pi$$

In addition, for any  $b_1, b_2 = 1, 2, 3, \dots$ , we always have

$$\int_0^{2\pi} \sin(b_1t) \cos(b_2t) dt = \frac{1}{2} \int_0^{2\pi} \sin(b_1t - b_2t) + \sin(b_1t + b_2t) dt = 0$$

Thus, only when  $b_1 = b_2$  we have

$$\int_0^{2\pi} \cos(c_1x + b_1t) \cos(c_2\rho x + b_2t) dt = \pi \cos(c_1x) \cos(c_2\rho x) + \pi \sin(c_1x) \sin(c_2\rho x) = \pi \cos((c_1 - c_2\rho)x)$$

Otherwise,  $\int_0^{2\pi} \cos(c_1x + b_1t) \cos(c_2\rho x + b_2t) dt = 0$ . Therefore, when  $b_1 = b_2$ , we have

$$\begin{aligned} & E(\cos(c_1x + b_1w) \cos(c_2y + b_2w)) \\ &= \frac{1}{2\pi} \frac{1}{\sqrt{2\pi}} e^{-\frac{c_2^2(1-\rho^2)}{2}} \int_0^{2\pi} \int_{-\infty}^{\infty} e^{-\frac{x^2}{2}} \cos(c_1x + b_1t) \cos(c_2\rho x + b_2t) dx dt \\ &= \frac{1}{2\pi} \frac{1}{\sqrt{2\pi}} e^{-\frac{c_2^2(1-\rho^2)}{2}} \int_{-\infty}^{\infty} e^{-\frac{x^2}{2}} \pi \cos((c_1 - c_2\rho)x) dx \\ &= \frac{1}{2\pi} \frac{1}{\sqrt{2\pi}} e^{-\frac{c_2^2(1-\rho^2)}{2}} \pi \sqrt{2\pi} e^{-(c_1 - c_2\rho)^2/2} \\ &= \frac{1}{2} e^{-\frac{c_1^2 + c_2^2 - 2c_1c_2\rho}{2}} \\ &= \frac{1}{2} e^{-c^2(1-\rho)}, \quad \text{when } c_1 = c_2 = c \end{aligned}$$

This completes the proof of the first moment. Next, using the following fact

$$\begin{aligned} E \cos(2cx + 2w) &= \frac{1}{2\pi} \int_0^{2\pi} \frac{1}{\sqrt{2\pi}} \int_{-\infty}^{\infty} \cos(2cx + 2t) e^{-x^2/2} dx dt \\ &= \frac{1}{2\pi} \int_0^{2\pi} \frac{1}{\sqrt{2\pi}} \frac{1}{2} \sin 2t \int_{-\infty}^{\infty} \cos(2cx) e^{-x^2/2} dx dt \\ &= \frac{1}{4\pi} e^{-2c^2} \int_0^{2\pi} \sin 2t dt = 0 \end{aligned}$$

we are ready to compute the second moment

$$\begin{aligned} & E[\cos(cx + w) \cos(cy + w)]^2 \\ &= \frac{1}{4} E[\cos(2cx + 2w) \cos(2cy + 2w) + \cos(2cx + 2w) + \cos(2cy + 2w)] + \frac{1}{4} \\ &= \frac{1}{4} E[\cos(2cx + 2w) \cos(2cy + 2w)] + \frac{1}{4} \\ &= \frac{1}{8} e^{-4c^2(1-\rho)} + \frac{1}{4} \end{aligned}$$

and the variance

$$\text{Var}[\cos(cx + w) \cos(cy + w)] = \frac{1}{8} e^{-4c^2(1-\rho)} + \frac{1}{4} - \frac{1}{4} e^{-2c^2(1-\rho)}$$



Finally, we prove the first moment without the “ $w$ ” random variable:

$$\begin{aligned}
& E(\cos(cx) \cos(cy)) \\
&= \int_{-\infty}^{\infty} \int_{-\infty}^{\infty} \cos(cx) \cos(cy) \frac{1}{2\pi} \frac{1}{\sqrt{1-\rho^2}} e^{-\frac{x^2+y^2-2\rho xy+\rho^2 x^2-\rho^2 y^2}{2(1-\rho^2)}} dx dy \\
&= \int_{-\infty}^{\infty} \frac{1}{2\pi} \frac{1}{\sqrt{1-\rho^2}} e^{-\frac{x^2}{2}} \cos(cx) dx \int_{-\infty}^{\infty} \cos(cy) e^{-\frac{(y-\rho x)^2}{2(1-\rho^2)}} dy \\
&= \int_{-\infty}^{\infty} \frac{1}{2\pi} e^{-\frac{x^2}{2}} \cos(cx) dx \int_{-\infty}^{\infty} \cos(cy \sqrt{1-\rho^2} + c\rho x) e^{-y^2/2} dy \\
&= \int_{-\infty}^{\infty} \frac{1}{2\pi} e^{-\frac{x^2}{2}} \cos(cx) \cos(c\rho x) dx \int_{-\infty}^{\infty} \cos(cy \sqrt{1-\rho^2}) e^{-y^2/2} dy \\
&= \int_{-\infty}^{\infty} \frac{1}{2\pi} e^{-\frac{x^2}{2}} \cos(cx) \cos(c\rho x) \sqrt{2\pi} e^{-c^2 \frac{1-\rho^2}{2}} dx \\
&= \frac{1}{\sqrt{2\pi}} e^{-c^2 \frac{1-\rho^2}{2}} \int_{-\infty}^{\infty} e^{-\frac{x^2}{2}} \cos(cx) \cos(c\rho x) dx \\
&= \frac{1}{\sqrt{2\pi}} e^{-c^2 \frac{1-\rho^2}{2}} \frac{\sqrt{2\pi}}{2} \left[ e^{-c^2 \frac{(1-\rho)^2}{2}} + e^{-c^2 \frac{(1+\rho)^2}{2}} \right] \\
&= \frac{1}{2} e^{-c^2(1-\rho)} + \frac{1}{2} e^{-c^2(1+\rho)}
\end{aligned}$$

This completes the proof of Theorem 2. □

**Proof of Theorem 3:** We will use some of the results from the proof of Theorem 2. Define

$$X_j = \sqrt{2} \cos(\sqrt{\gamma} x_j + w_j), \quad Y_j = \sqrt{2} \cos(\sqrt{\gamma} y_j + w_j), \quad Z_k = \frac{\sum_{j=1}^k X_j Y_j}{\sqrt{\sum_{j=1}^k X_j^2} \sqrt{\sum_{j=1}^k Y_j^2}}$$

From Theorem 2, it is easy to see that, as  $k \rightarrow \infty$ , we have

$$\frac{1}{k} \sum_{j=1}^k X_j^2 \rightarrow E(X_j^2) = e^{-\gamma(1-1)} = 1, \quad a.s. \quad \frac{1}{k} \sum_{j=1}^k Y_j^2 \rightarrow 1, \quad a.s.$$

and

$$Z_k = \frac{\frac{1}{k} \sum_{j=1}^k X_j Y_j}{\sqrt{\frac{1}{k} \sum_{j=1}^k X_j^2} \sqrt{\frac{1}{k} \sum_{j=1}^k Y_j^2}} \rightarrow e^{-\gamma(1-\rho)} = Z_{\infty}, \quad a.s.$$

We express the deviation  $Z_k - Z_\infty$  as

$$\begin{aligned}
Z_k - Z_\infty &= \frac{\frac{1}{k} \sum_{j=1}^k X_j Y_j - Z_\infty + Z_\infty}{\sqrt{\frac{1}{k} \sum_{j=1}^k X_j^2} \sqrt{\frac{1}{k} \sum_{j=1}^k Y_j^2}} - Z_\infty \\
&= \frac{\frac{1}{k} \sum_{j=1}^k X_j Y_j - Z_\infty}{\sqrt{\frac{1}{k} \sum_{j=1}^k X_j^2} \sqrt{\frac{1}{k} \sum_{j=1}^k Y_j^2}} + Z_\infty \frac{1 - \sqrt{\frac{1}{k} \sum_{j=1}^k X_j^2} \sqrt{\frac{1}{k} \sum_{j=1}^k Y_j^2}}{\sqrt{\frac{1}{k} \sum_{j=1}^k X_j^2} \sqrt{\frac{1}{k} \sum_{j=1}^k Y_j^2}} \\
&= \frac{1}{k} \sum_{j=1}^k X_j Y_j - Z_\infty + Z_\infty \frac{1 - \frac{1}{k} \sum_{j=1}^k X_j^2 \frac{1}{k} \sum_{j=1}^k Y_j^2}{2} + O_P(1/k) \\
&= \frac{1}{k} \sum_{j=1}^k X_j Y_j - Z_\infty + Z_\infty \frac{1 - \frac{1}{k} \sum_{j=1}^k X_j^2}{2} + Z_\infty \frac{1 - \frac{1}{k} \sum_{j=1}^k Y_j^2}{2} + O_P(1/k)
\end{aligned}$$

Note that if  $a \approx 1$  and  $b \approx 1$ , then

$$1 - ab = 1 - (1 - (1 - a))(1 - (1 - b)) = (1 - a) + (1 - b) - (1 - a)(1 - b)$$

and we can ignore the higher-order term.

Therefore, to analyze the asymptotic variance, it suffices to study the following expectation

$$\begin{aligned}
&E \left( XY - Z_\infty + Z_\infty \frac{1 - X^2}{2} + Z_\infty \frac{1 - Y^2}{2} \right)^2 \\
&= E \left( XY - Z_\infty (X^2 + Y^2)/2 \right)^2 \\
&= E(X^2 Y^2) + Z_\infty^2 E(X^4 + Y^4 + 2X^2 Y^2)/4 - Z_\infty E(X^3 Y) - Z_\infty E(X Y^3)
\end{aligned}$$

which can be obtained from the results in the proof of Theorem 2. In particular, if  $b_1 = b_2$ , then

$$E(\cos(c_1 x + b_1 w) \cos(c_2 y + b_2 w)) = \frac{1}{2} e^{-\frac{c_1^2 + c_2^2 - 2c_1 c_2 \rho}{2}}$$

Otherwise  $E(\cos(c_1 x + b_1 w) \cos(c_2 y + b_2 w)) = 0$ . We can now compute

$$\begin{aligned}
&E[\cos(cx + w)^3 \cos(cy + w)] \\
&= E\left[\frac{1}{4} \cos(3(cx + w)) \cos(cy + w) + \frac{3}{4} \cos(cx + w) \cos(cy + w)\right] \\
&= \frac{3}{8} e^{-c^2(1-\rho)}
\end{aligned}$$

$$E[\cos(cx + w) \cos(cy + w)]^2 = \frac{1}{8} e^{-4c^2(1-\rho)} + \frac{1}{4}$$

$$E[\cos(cx + w)]^4 = \frac{1}{8} + \frac{1}{4} = \frac{3}{8}$$

$$\begin{aligned}
V_{n,\rho,\gamma} &= E \left( XY - Z_\infty + Z_\infty \frac{1-X^2}{2} + Z_\infty \frac{1-Y^2}{2} \right)^2 \\
&= E(X^2Y^2) + Z_\infty^2 E(X^4 + Y^4 + 2X^2Y^2)/4 - Z_\infty E(X^3Y) - Z_\infty E(XY^3) \\
&= \frac{1}{2}e^{-4c^2(1-\rho)} + 1 + e^{-2c^2(1-\rho)} \left( \frac{3}{8} + \frac{3}{8} + \frac{1}{4}e^{-4c^2(1-\rho)} + \frac{1}{2} \right) - e^{-c^2(1-\rho)} \left( \frac{3}{2}e^{-c^2(1-\rho)} + \frac{3}{2}e^{-c^2(1-\rho)} \right) \\
&= \frac{1}{2}e^{-4c^2(1-\rho)} + 1 + e^{-2c^2(1-\rho)} \left( \frac{5}{4} + \frac{1}{4}e^{-4c^2(1-\rho)} \right) - 3e^{-2c^2(1-\rho)} \\
&= \frac{1}{2}e^{-4c^2(1-\rho)} + 1 + \frac{1}{4}e^{-6c^2(1-\rho)} - \frac{7}{4}e^{-2c^2(1-\rho)} \\
&= V_{\rho,\gamma} - \frac{1}{4}e^{-2c^2(1-\rho)} \left[ 3 - e^{-4c^2(1-\rho)} \right]
\end{aligned}$$

where  $V_{\rho,\gamma}$  is the corresponding variance factor without using normalization:

$$V_{\rho,\gamma} = \frac{1}{2} + \frac{1}{2} \left( 1 - e^{-2c^2(1-\rho)} \right)^2$$

This completes the proof of Theorem 3. □

### 3 An Experimental Study on Kernel SVMs

Table 1 lists 25 publicly available datasets, from the UCI repository and the LIBSVM website, for our experimental study, along with the kernel SVM classification results for the RBF kernel and the proposed GMM kernel, at the best  $l_2$ -regularization  $C$  values. More detailed results (for all regularization  $C$  values) are available in Figures 4 and 5. To ensure repeatability, we use the LIBSVM pre-computed kernel functionality. This also means we can not (easily) test nonlinear kernels on larger datasets (but then we can resort to hashing, GMM or RFF, and linear algorithms).

For the RBF kernel, we exhaustively experimented with 58 different values of  $\gamma \in \{0.001, 0.01, 0.1:0.1:2, 2.5, 3:1:20, 25:5:50, 60:10:100, 120, 150, 200, 300, 500, 1000\}$ . Basically, Table 1 reports the best RBF results among all  $\gamma$  and  $C$  values in our experiments.

The classification results in Table 1 and Figures 4 and 5 indicate that, on these datasets, kernel (GMM and RBF) SVM classifiers improve over linear classifiers substantially. For most datasets, the GMM kernel (which has no tuning parameter) outperforms the best-tuned RBF kernel. For a small number of datasets (e.g., “SEMG1”), even though the RBF kernel performs better, we will show in Section 4 that the GCWS hashing can still be substantially better than the RFF hashing.

Table 1: **25 public datasets and kernel SVM results.** We report the test classification accuracies for linear kernel, RBF kernel (with the best  $\gamma$  value in parentheses), and GMM kernel, at the best SVM regularization  $C$  values. Note that the last four datasets are too large for using pre-computed kernel functionality and hence only the linear SVM results are reported.

Dataset	# train	# test	# dim	linear (%)	RBF ( $\gamma$ ) (%)	GMM (%)
DailySports	4560	4560	5625	77.7	97.6 (6)	<b>99.6</b>
Fourclass	431	431	2	72.6	81.2 (45)	<b>100</b>
IJCNN5k	5000	91701	22	91.9	<b>95.8</b> (9)	95.1
Letter	15000	5000	16	61.7	<b>97.4</b> (11)	97.3
MSD20k	20000	20000	90	66.7	68.0 (0.9)	<b>71.1</b>
Musk	3299	3299	166	95.1	<b>99.3</b> (1.2)	99.2
PAMAP101	20000	20000	51	76.9	94.3 (1.5)	<b>98.9</b>
PAMAP102	20000	20000	51	81.2	95.7 (0.5)	<b>98.8</b>
PAMAP103	20000	20000	51	85.5	97.5 (0.5)	<b>99.7</b>
PAMAP104	20000	20000	51	84.0	97.3 (19)	<b>99.3</b>
PAMAP105	20000	20000	51	79.4	97.3 (18)	<b>99.2</b>
Satimage	2218	2217	36	80.5	90.5 (8)	<b>91.5</b>
Segment	1155	1155	19	92.7	97.0 (0.5)	<b>97.8</b>
SEMG1	900	900	3000	26.0	<b>43.6</b> (4)	41.0
SEMG2	1800	1800	2500	19.3	29.0 (6)	<b>54.0</b>
SensIT20k	20000	19705	100	80.4	83.2 (0.1)	<b>84.6</b>
Sensorless	29255	29254	48	61.5	93.0 (0.4)	<b>99.4</b>
Shuttle500	500	43000	9	93.4	99.0 (90)	<b>99.6</b>
SVMGuide1	3089	4000	4	79.9	90.6 (50)	<b>97.3</b>
USPS	7291	2007	256	91.6	<b>95.7</b> (4)	95.0
Vowel	528	462	10	27.9	48.1 (13)	<b>62.8</b>
IJCNN	49990	91701	22	92.6	– (9)	–
PAMAP101Large	186581	186580	51	79.2	– (1.5)	–
PAMAP105Large	185548	185548	51	83.4	– (18)	–
SensIT	78823	19705	100	80.5	– (0.1)	–

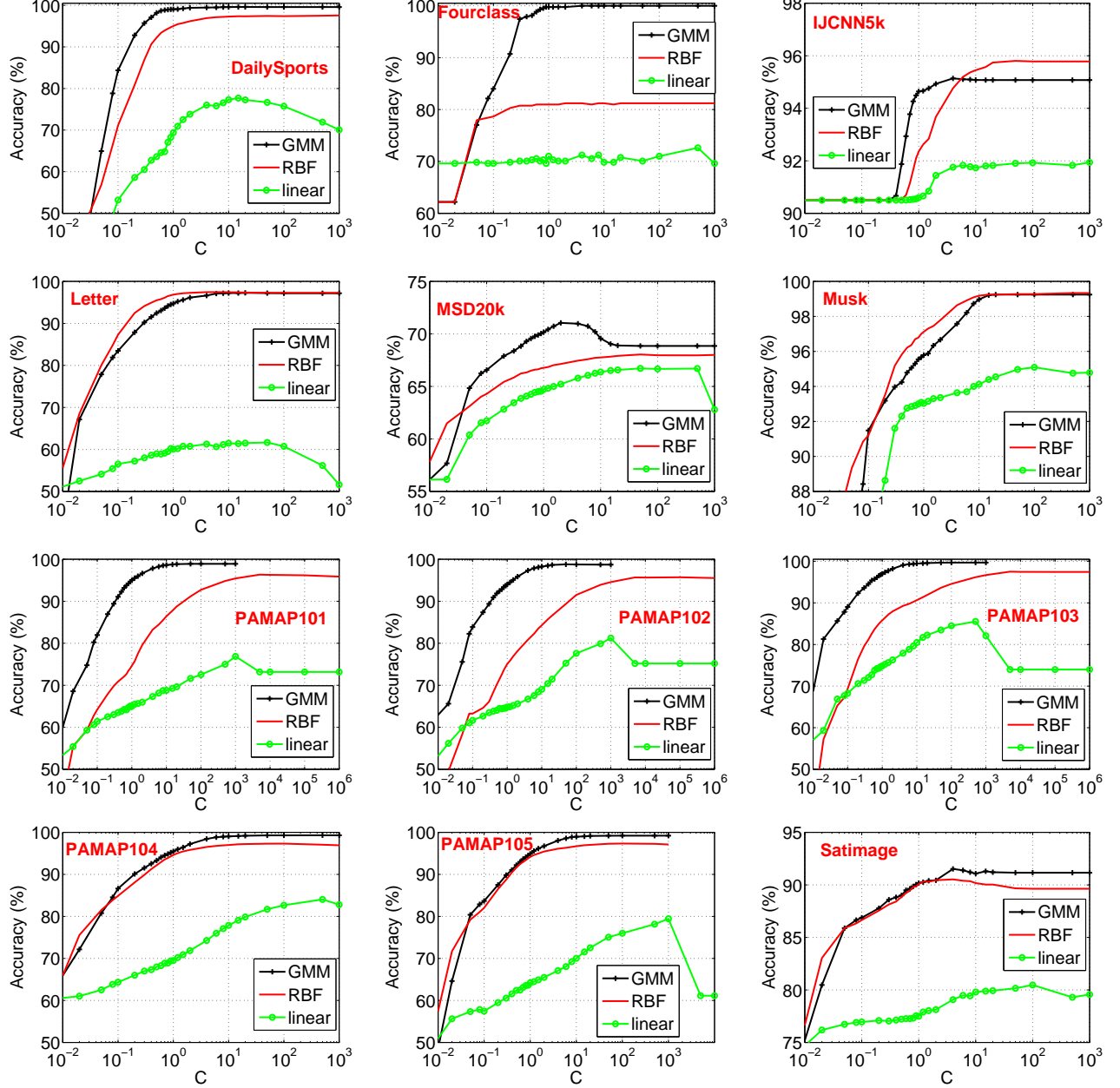


Figure 4: **Test classification accuracies using kernel SVMs.** Both the GMM kernel and RBF kernel substantially improve linear SVM.  $C$  is the  $l_2$ -regularization parameter of SVM. For the RBF kernel, we report the result at the best  $\gamma$  value for every  $C$  value.

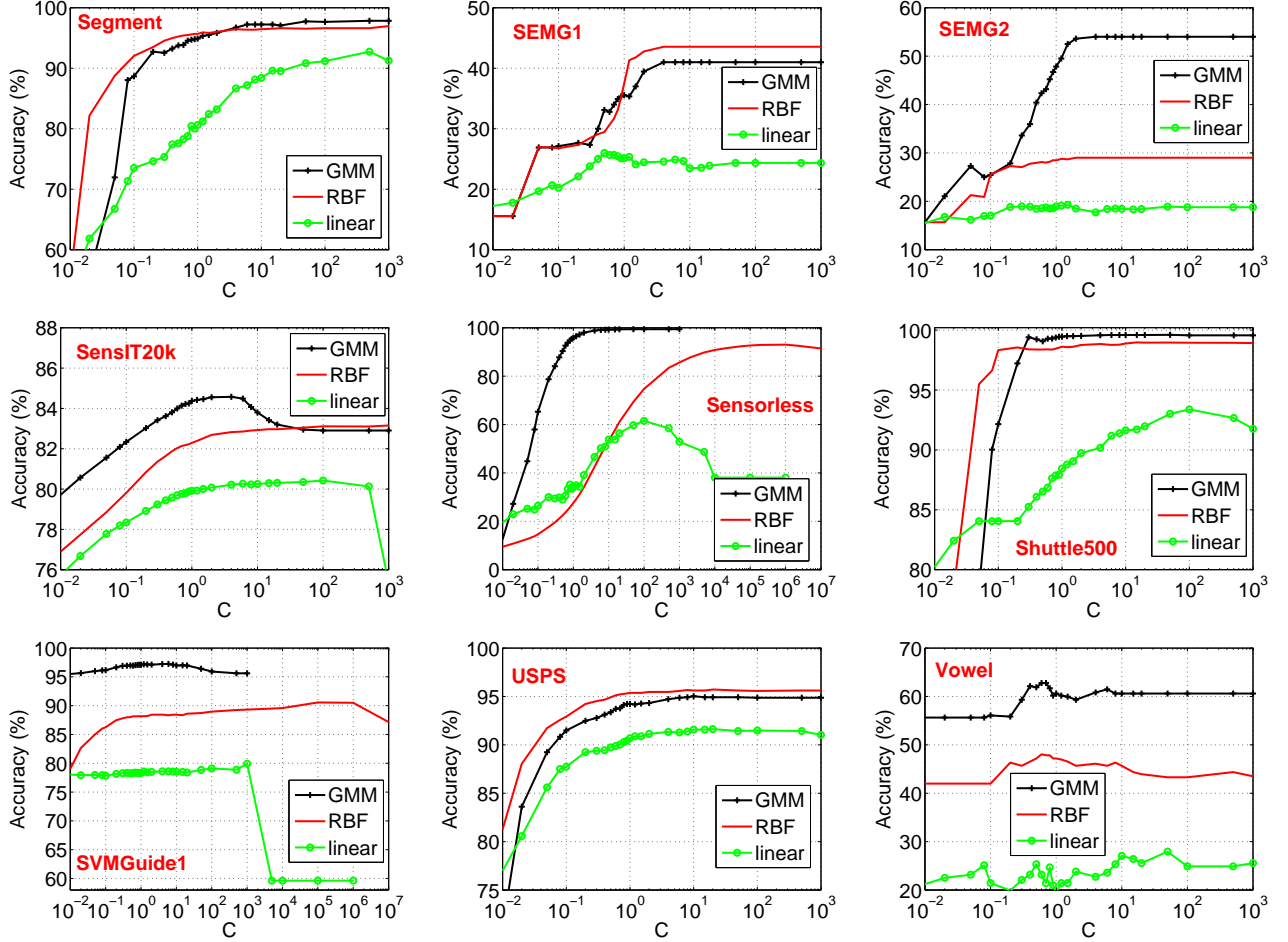


Figure 5: **Test classification accuracies using kernel SVMs.** Both the GMM kernel and RBF kernel substantially improve linear SVM.  $C$  is the  $l_2$ -regularization parameter of SVM. For the RBF kernel, we report the result at the best  $\gamma$  value for every  $C$  value.

## 4 Hashing for Linearization of Nonlinear Kernels

It is known that a straightforward implementation of nonlinear kernels can be difficult for large datasets [3]. For example, for a small dataset with merely 60,000 data points, the  $60,000 \times 60,000$  kernel matrix has  $3.6 \times 10^9$  entries. In practice, being able to linearize nonlinear kernels becomes very beneficial, as that would allow us to easily apply efficient linear algorithms especially online learning [2]. Randomization (hashing) is a popular tool for kernel linearization.

In the introduction, we have explained how to linearize both the RBF kernel and the GMM kernel. From practitioner’s perspective, while the kernel classification results in Table 1 are informative, they are not sufficient for guiding the choice of kernels. For example, as we will show, for some datasets, even though the RBF kernel performs better than the GMM kernel, the linearization algorithm (i.e., the normalized RFF) requires substantially more samples (i.e., larger  $k$ ).

Note that in our SVM experiments, since we always normalize the input features to the unit  $l_2$  norm, we do not always explicit say “normalized RFF” (or NRFF).

Figure 6 reports the test classification accuracies on the **Letter** dataset, for both linearized GMM kernel using GCWS and linearized RBF kernel (at the best  $\gamma$ ) using RFF, using LIBLINEAR. From Table 1, we can see that the original RBF kernel slightly outperforms the GMM kernel. Very interestingly, the results obtained by GCWS hashing and linear classification are noticeably better than the results of (normalized) RFF hashing and linear classification, especially when the number of samples ( $k$ ) is not too large (i.e., the right panels).

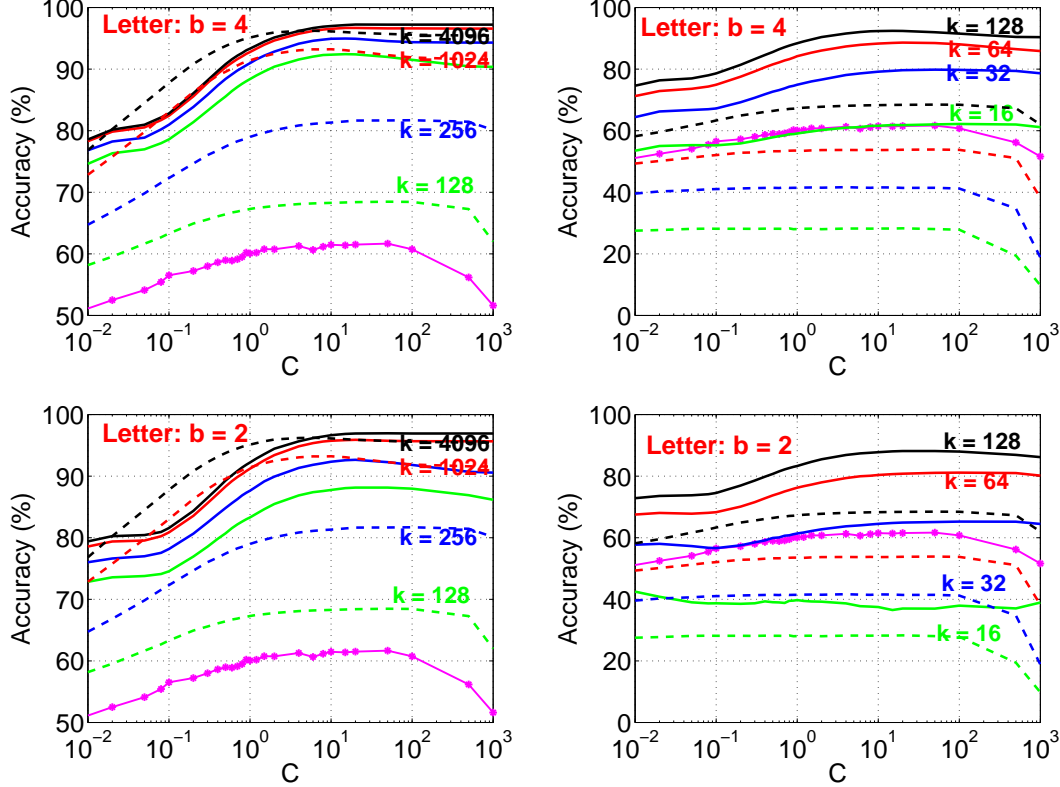


Figure 6: **Letter**: Test classification accuracies of the linearized GMM kernel (solid) and linearized RBF (dashed) kernel, using LIBLINEAR, averaged over 10 repetitions. In each panel, we report the results on 4 different  $k$  (sample size) values: 128, 256, 1024, 4096 (left panels), and 16, 32, 64, 128 (right panels). We can see that the linearized RBF (using RFF) would require substantially more samples in order to reach the same accuracies as the linearized GMM kernel (using GCWS). Two interesting points: (i) Although the original (best-tuned) RBF kernel slightly outperforms the original GMM kernel, the results of GCWS are still more accurate than the results of RFF even at  $k = 4096$ , which is very large, especially considering the original data dimension is merely 16. (ii) The right panels show that with merely  $k = 16$  samples ( $b = 4$ ), GCWS already produces better results than linear SVM based on the original dataset (the solid curve marked by \*).

For the “Letter” dataset, the original dimension is merely 16 (and  $b = 4$  would be sufficient to represent the hashed values). It is known that, for modern linear algorithms, the computational cost is largely determined by the number of nonzeros. Hence the number of samples (i.e.,  $k$ ) is a crucial parameter which directly controls the training complexity. From the right panels of Figure 6, we can see that with merely  $k = 16$  samples, GCWS already produces better results than the original linear method. This phenomenon is exciting, because in industrial practice, the goal is often to produce better results than linear methods without consuming much more resources.

Figure 7 reports the test classification accuracies on the **DailySports** dataset, for both linearized GMM kernel using GCWS and linearized RBF kernel (at the best  $\gamma$ ) using RFF. From Table 1, we can see that the original GMM kernel slightly outperforms the RBF kernel. The performance gap is significantly magnified in the linearization results. We can also see that the parameter  $b$  (i.e., the number of bits we store for each GCWS hashed value  $i^*$ ) does matter. Nevertheless, as long as  $b \geq 4$ , the results do not appear to differ much in this case.

Figure 8 reports the test classification accuracies on the **SEMG1** and **SEMG2** datasets. For the SEMG2 dataset, we can see that the linearized GMM kernel substantially outperforms the linearized RBF kernel, which is expected, because as shown in Table 1 the original GMM kernel significantly outperforms the original RBF kernel. The results on the SEMG1 dataset are perhaps more interesting. For SEMG1, the original RBF kernel actually outperforms the original GMM kernel. Nevertheless, after linearization, the results of GCWS are still substantially more accurate than the results of RFF at the same  $k$ .

Figure 9 reports the test classification accuracies on the **PAMAP101** and **PAMAP103** datasets. For both datasets, the linearized GMM kernel substantially outperforms the linearized RBF kernel. The results for  $b = 4$  do not differ much from the results for  $b = 8$ .

Figure 10 reports the test classification accuracies on the **Musk** and **IJCNN5k** datasets. For these two datasets, the original RBF kernel actually outperforms the original GMM kernel. Nevertheless, GCWS significantly outperforms RFF, except for “Musk” and  $k = 4096$ .

Figure 11 reports the test classification accuracies on four larger datasets for which we can not directly compute kernel SVM classifiers. We can still compute linear classifiers on the original (solid curves marked by \*) and on the hashed data by GCWS or RFF. The results show that (i) hashing + linear classifiers is a good strategy for building accurate statistical models on large data; and (ii) on these four datasets, GCWS performs substantially better than RFF.

In summary, linearization via GCWS works well for the GMM kernel. In contrast, the random Fourier feature (RFF) approach typically requires substantially more samples (i.e., much larger  $k$ ). This phenomenon can be in part explained by Theorem 2 which says that the variance of RFF has a constant term which does not vanish (unless the sample size  $k$  is very large).



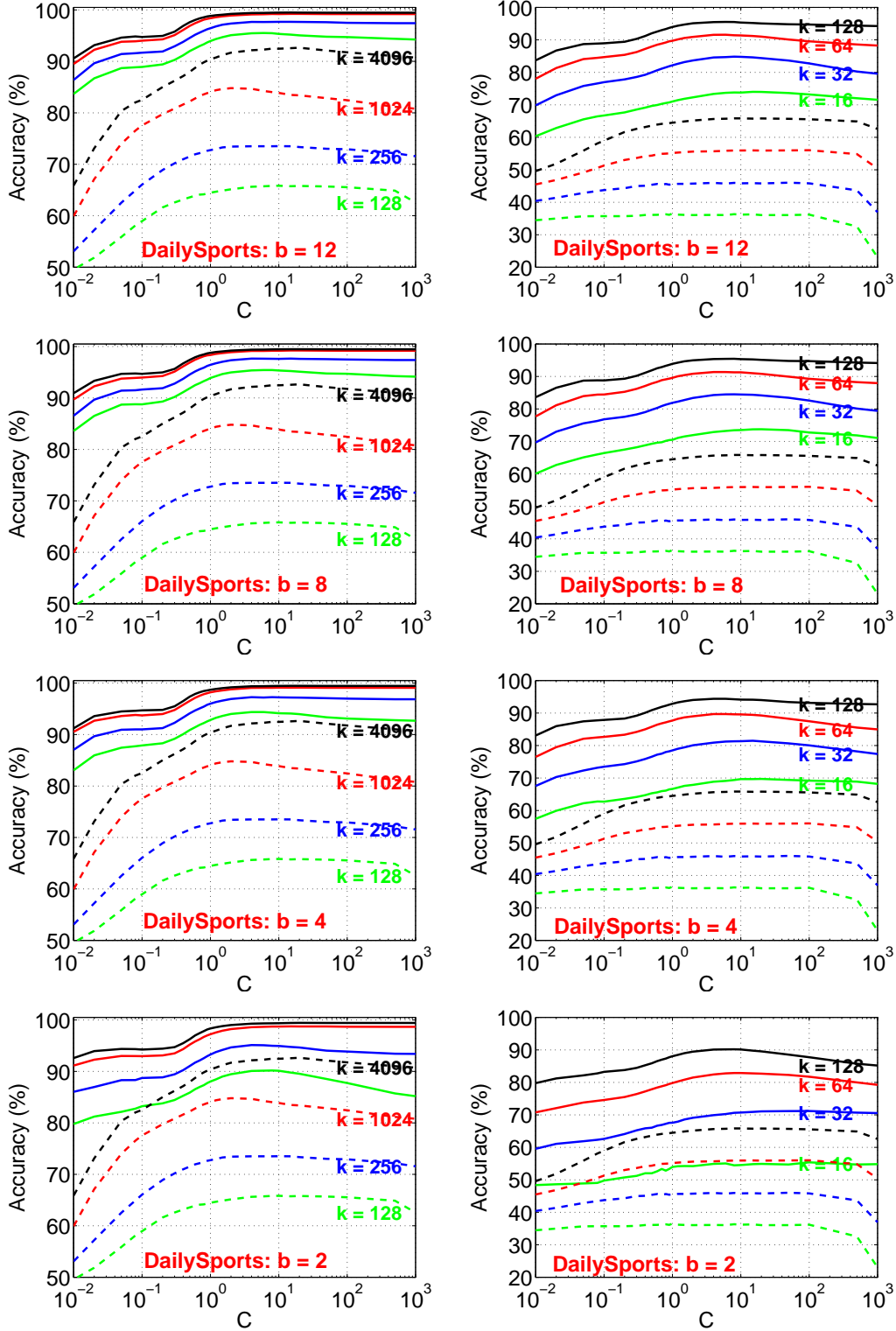


Figure 7: **DailySports**: Test classification accuracies of the linearized GMM kernel (solid) and linearized RBF (dashed) kernel, using LIBLINEAR. In each panel, we report the results on 4 different  $k$  (sample size) values: 128, 256, 1024, 4096 (left panels), and 16, 32, 64, 128 (right panels). We can see that the linearized RBF (using RFF) would require substantially more samples in order to reach the same accuracies as the linearized GMM kernel (using GCWS).

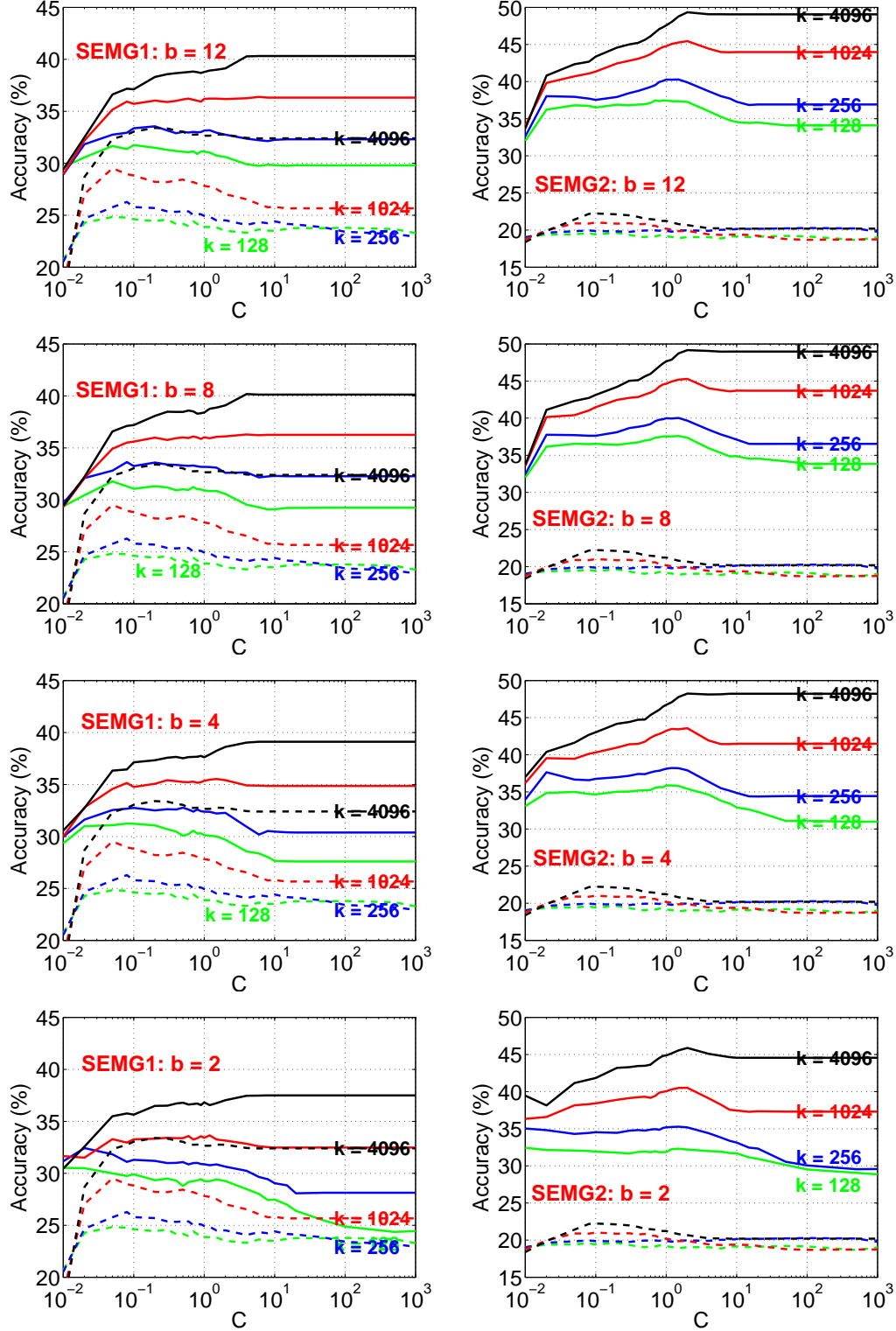


Figure 8: **SEMG1 and SEMG2**: Test classification accuracies of the linearized GMM kernel (solid) and linearized RBF (dashed) kernel, using LIBLINEAR. Again, we can see that the linearized RBF would require substantially more samples in order to reach the same accuracies as the linearized GMM kernel. Note that, for SEMG1, the original RBF kernel actually outperforms the original GMM kernel as shown in Table 1.

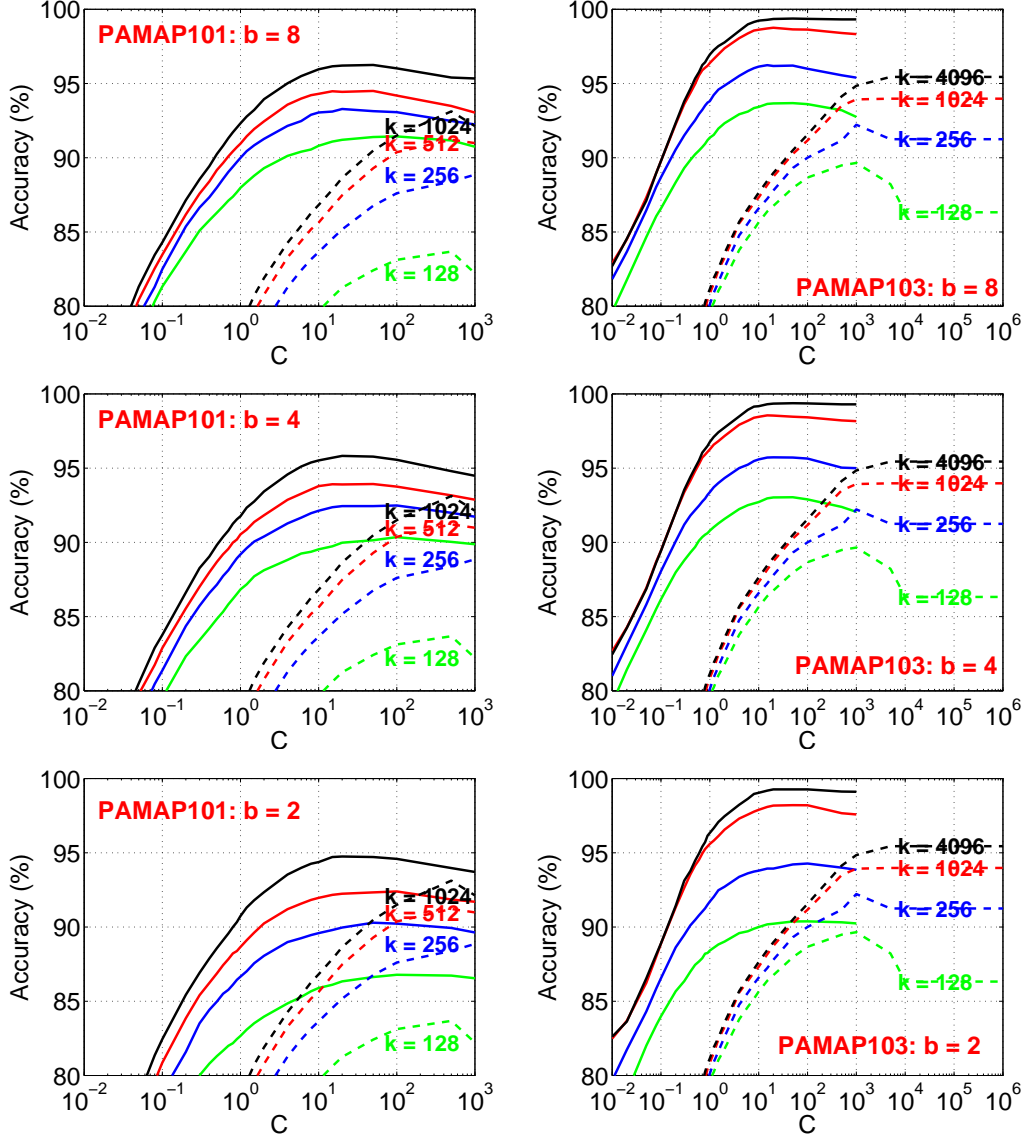


Figure 9: **PAMAP101 and PAMAP103**: Test classification accuracies of the linearized GMM kernel (solid) and linearized RBF (dashed) kernel, using LIBLINEAR. For these two datasets, the linearized RBF would require substantially more samples in order to reach the same accuracies as the linearized GMM kernel.

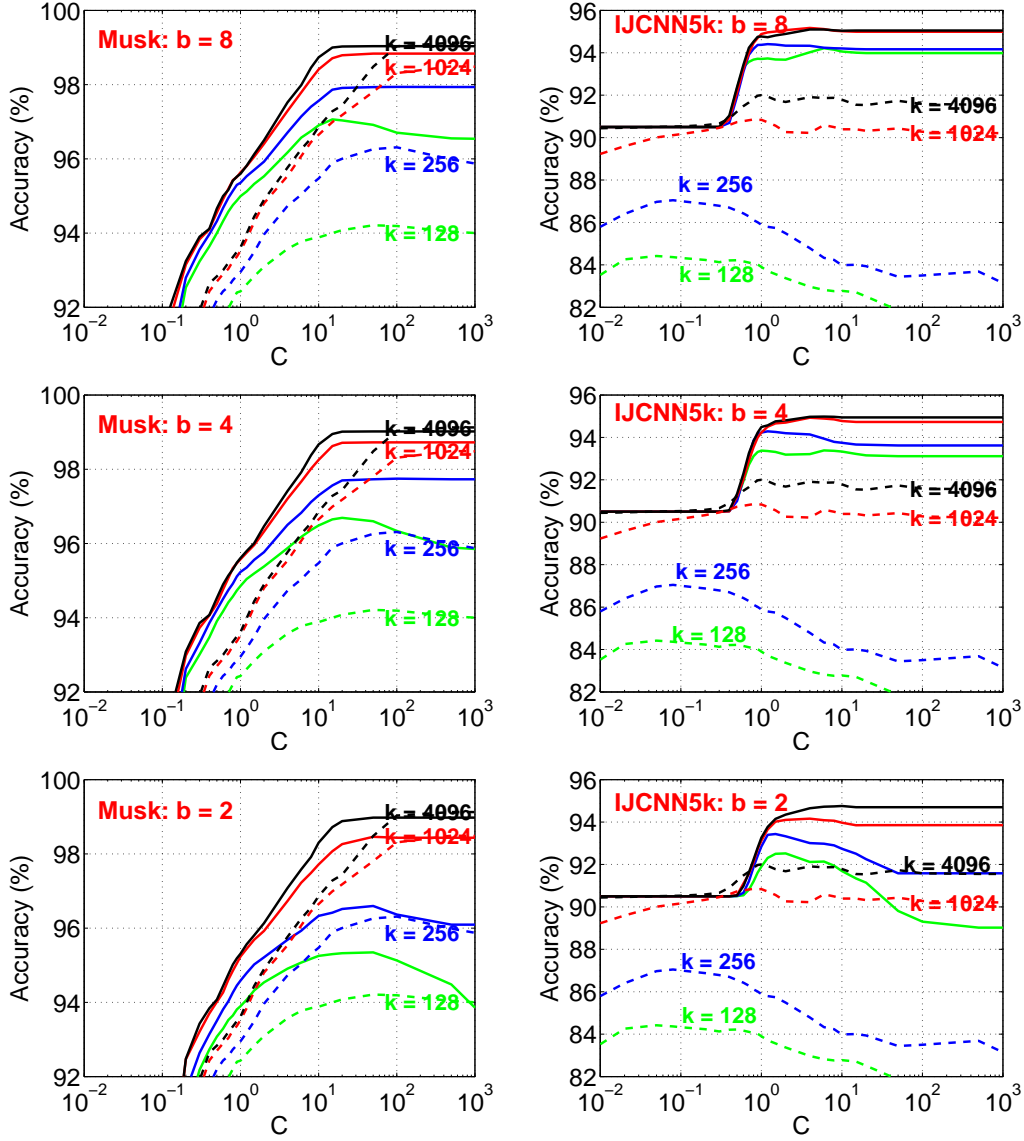


Figure 10: **Musk** and **IJCNN5k**: Test classification accuracies of the linearized GMM kernel (solid) and linearized RBF (dashed) kernel, using LIBLINEAR. For these two datasets, the original RBF kernel actually outperforms the original GMM kernel. Nevertheless, GCWS significantly outperforms RFF, except for “Musk” and  $k = 4096$ .

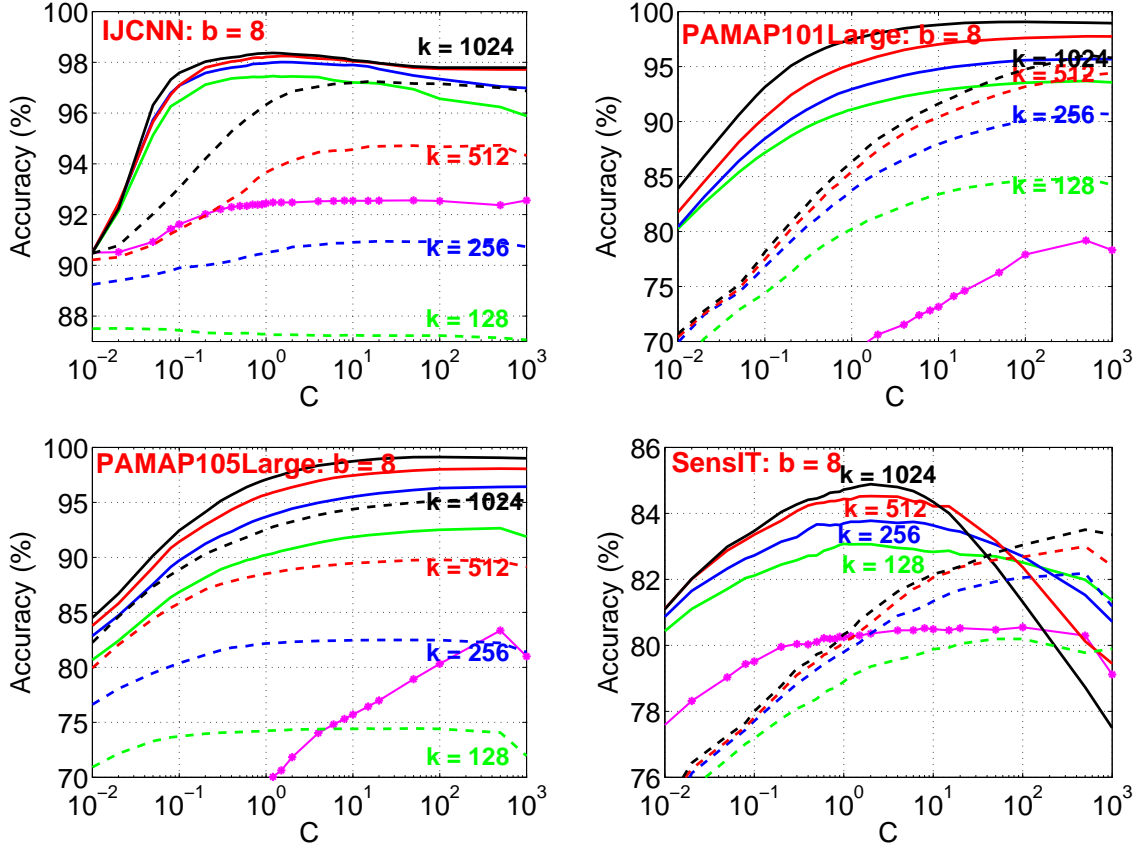


Figure 11: **Larger datasets:** Test classification accuracies of the linearized GMM kernel (solid) and linearized RBF (dashed) kernel, using LIBLINEAR, on four larger datasets which we can not directly compute kernel SVM classifiers. Nevertheless, we can still computer linear classifiers on the original (solid curves marked by \*) and on the hashed data.

**Training time:** For linear algorithms, the training cost is largely determined by the number of nonzero entries per input data vector. In other words, at the same  $k$ , the training times of GCWS and RFF will be roughly comparable. For GCWS and batch algorithms (such as LIBLINEAR), a larger  $b$  will increase the training time but not much. See Figure 12 for an example, which actually shows that RFF will consume more time at high  $C$  (for good accuracy). Note that, with online learning, it would be more obvious that the training time is determined by the number of nonzeros and number of epochs (for industrial practice, typically only one epoch or a few epoches are used).

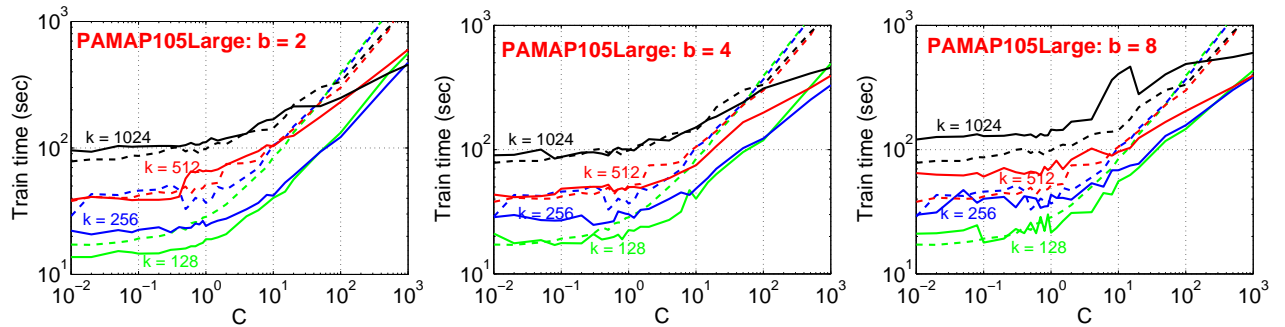


Figure 12: **PAMAP105Large:** Training times of GCWS (solid curves) and RFF (dashed curves), for four sample sizes  $k \in \{128, 256, 512, 1024\}$ , and  $b \in \{2, 4, 8\}$ .

## 5 Kernels and Hashing on Nonnegative Data

In practice, it is fairly common to encounter nonnegative data. Here, we also provide a set of experiments on 25 public nonnegative datasets in Table 2, to compare GMM with RBF, fRBF (folded RBF), and linear methods, as well as their corresponding hashing methods (GCWS and RFF). Here the folded RBF kernel is defined in (11):

$$fRBF(u, v; \gamma) = \frac{1}{2}e^{-\gamma(1-\rho)} + \frac{1}{2}e^{-\gamma(1+\rho)}$$

which is monotonic in  $\rho \geq 0$ . Note that for nonnegative data, GMM becomes the original min-max kernel. The kernel SVM classification results (at the best regularization  $C$  and tuning parameter  $\gamma$ ) are reported in Table 2 and Figure 13.

One motivation for developing the fRBF kernel is to address the concern that the original min-max kernel is designed for nonnegative data while the original RBF kernel is for general data. Another motivation is for simplifying the sampling procedure of RFF by removing the random variable  $w$  in the procedure.

The kernel SVM classification results are reported in Table 2 and Figure 13. The results show that the nonlinear kernels typically substantially improve over linear classifiers. The fRBF kernel performs very similarly to RBF. For about half of the datasets, the GMM outperforms the best tuned RBF and fRBF kernels.

Figure 14 compares the hashing method for RBF (i.e., RFF) with the hashing method for fRBF (i.e., RFF without using  $w$ ). We can see that the two perform very similarly, justifying the removal of the random variable  $w$  in the procedure.

Figure 15 compares the classification results of GCWS (solid curves) and RFF (dashed curves), for selected datasets. Clearly, RBF requires substantially more samples. For the “M-Rotate” dataset, the original RBF kernel notably outperforms the original min-max kernel (89.7% versus 84.8%). However, as shown in Figure 15, even with 4096 samples, the accuracy of RFF is still substantially lower than the accuracy of GCWS.

The “WebspamN1” dataset (bottom right panel) is too large for using the LIBSVM pre-computed kernel functionality in common workstations. Nevertheless, we can easily hash the nonlinear kernels and run LIBLINEAR on the transformed dataset. The corresponding plot of Figure 15 again confirms that, on this dataset, GCWS requires substantially fewer samples than RFF in order to reach the same accuracy.

Table 2: **25 public nonnegative datasets.** The data are public (and mostly well-known), from various sources including the UCI repository, the LIBSVM web site, the web site for the book [7], and the papers [11, 12, 13]. Whenever possible, we use the conventional partitions of training and testing sets. We reports the best SVM classification results (at the best  $C$  value), for four different kernels: linear, RBF, folded RBF (fRBF), and GMM.

Dataset	# train	# test	# dim	linear (%)	RBF ( $\gamma$ ) (%)	fRBF ( $\gamma$ ) (%)	GMM (%)
Coverttype10k	10000	50000	54	70.9	80.1 (120)	80.1 (100)	<b>80.4</b>
Coverttype20k	20,000	50000	54	71.1	<b>83.8</b> (150)	<b>83.8</b> (150)	83.3
Isolet	6238	1559	617	95.5	96.8 (6)	<b>96.9</b> (11)	96.4
M-Basic	12000	50000	784	90.0	<b>97.2</b> (5)	<b>97.2</b> (5)	96.2
M-Image	12000	50000	784	70.7	77.8 (16)	77.8 (16)	<b>80.8</b>
MNIST10k	10000	60000	784	90.0	96.8 (5)	<b>96.9</b> (5)	95.7
M-Noise1	10000	4000	784	60.3	66.8 (10)	66.8 (10)	<b>71.4</b>
M-Noise2	10000	4000	784	62.1	69.2 (11)	69.2 (11)	<b>72.4</b>
M-Noise3	10000	4000	784	65.2	71.7 (11)	71.7 (11)	<b>73.6</b>
M-Noise4	10000	4000	784	68.4	75.3 (14)	75.3 (14)	<b>76.1</b>
M-Noise5	10000	4000	784	72.3	78.7 (12)	78.6 (11)	<b>79.0</b>
M-Noise6	10000	4000	784	78.7	<b>85.3</b> (15)	<b>85.3</b> (15)	84.2
M-Rand	12000	50000	784	78.9	<b>85.4</b> (12)	<b>85.4</b> (12)	84.2
M-Rotate	12000	50000	784	48.0	<b>89.7</b> (5)	<b>89.7</b> (5)	84.8
M-RotImg	12000	50000	784	31.4	<b>45.8</b> (18)	<b>45.8</b> (18)	41.0
Optdigits	3823	1797	64	95.3	<b>98.7</b> (8)	<b>98.7</b> (8)	97.7
Pendigits	7494	3498	16	87.6	<b>98.7</b> (13)	<b>98.7</b> (11)	97.9
Phoneme	3340	1169	256	91.4	92.4 (10)	<b>92.5</b> (9)	<b>92.5</b>
Protein	17766	6621	357	69.1	70.3 (4)	70.2 (4)	<b>72.4</b>
RCV1	20242	60000	47236	96.3	96.7 (1.7)	96.7 (0.3)	<b>96.9</b>
Spam	3065	1536	54	92.6	94.6 (1.2)	94.6 (1.7)	<b>95.0</b>
Splice	1000	2175	60	85.1	90.0 (15)	89.8 (16)	<b>95.2</b>
WebspamN1-20k	20000	60000	254	93.0	<b>98.0</b> (35)	<b>98.0</b> (35)	97.9
YoutubeVision	11736	10000	512	62.3	70.2 (3)	70.1 (4)	<b>72.2</b>
WebspamN1	175000	175000	254	93.3	– (35)	– (35)	–

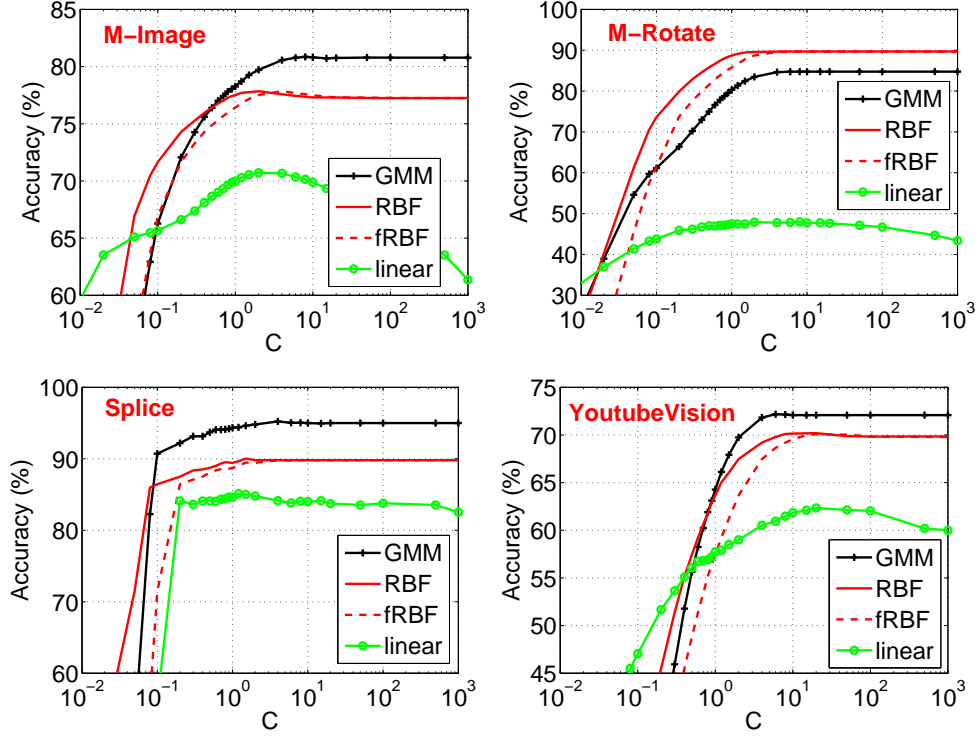


Figure 13: Test classification accuracies for nonlinear kernels using  $l_2$ -regularized SVM. For RBF/fRBF kernels, at each  $C$ , we report the best accuracy from the results among all  $\gamma$  values. For comparison, we also include linear SVM results (green if color is available).

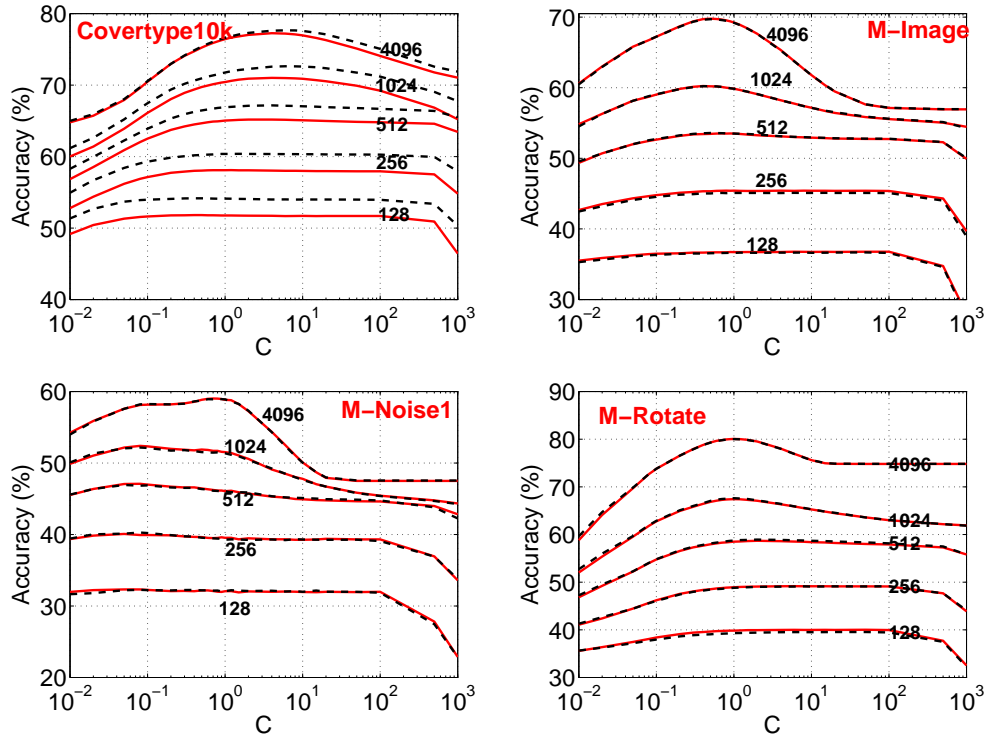


Figure 14: Classification accuracies of the linearized RBF (solid curves) and linearized fRBF (dashed curves) kernels, using LIBLINEAR. Both RBF and fRBF perform almost identically.



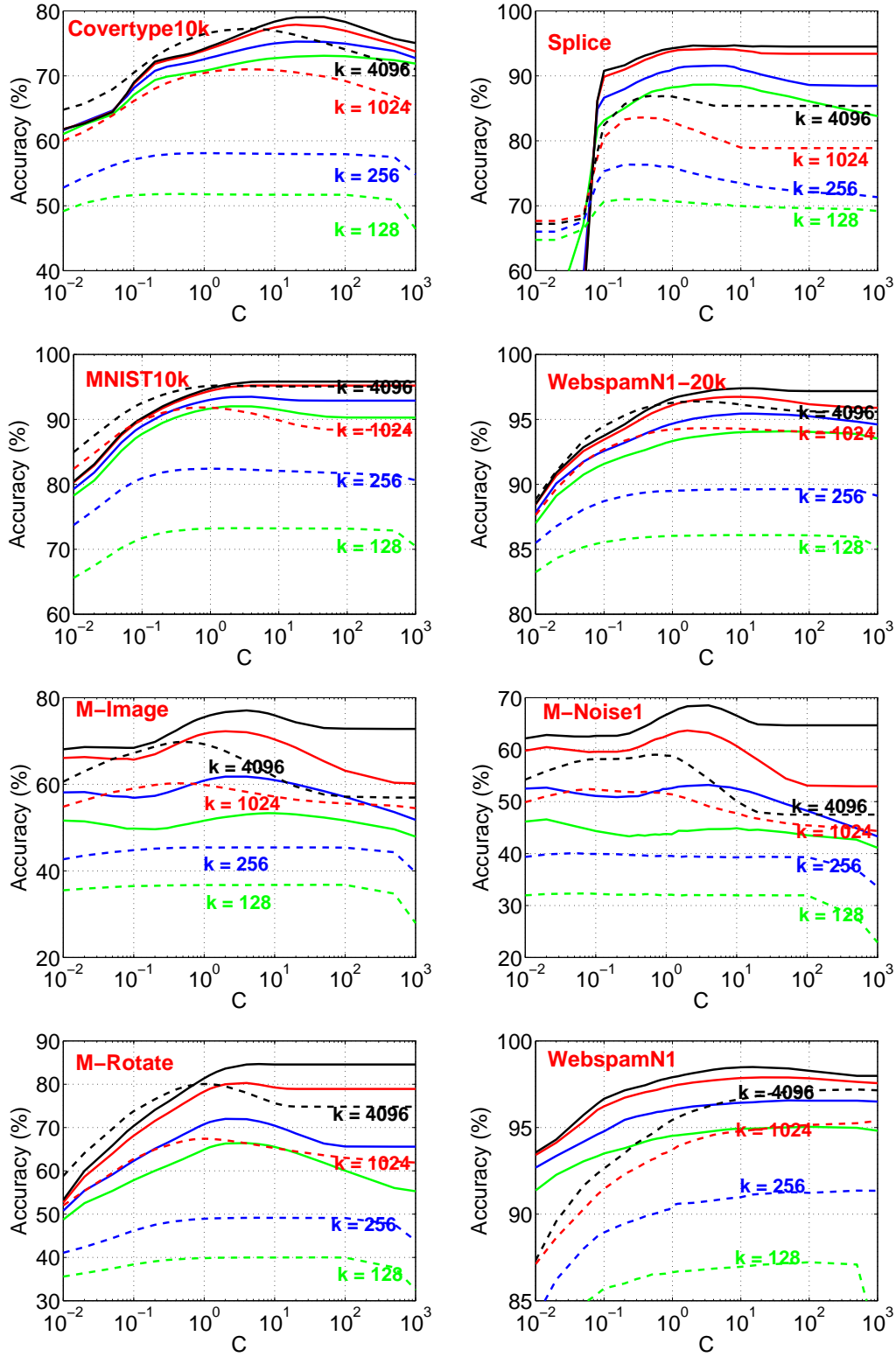


Figure 15: Classification accuracies of GCWS (solid curves) and RFF (dashed curves) kernel, using LIBLINEAR. We report the results on 4 different  $k$  (sample size) values. We can see that RFF would require substantially more samples in order to reach the same accuracies as GCWS.

## 6 Conclusion

Large-scale machine learning has become increasingly important in practice. For many industrial applications, typically only linear methods are affordable, and it is practically beneficial to have methods which can provide substantially more accurate prediction results than linear methods, with no essential increase of the computation cost. The method of “random Fourier features” (RFF) has been a very popular tool for linearizing the radial basis function (RBF) kernel, with numerous applications in machine learning, computer vision, and beyond, e.g., [21, 27, 1, 8, 5, 28, 9, 25, 4, 23].

In this paper, we propose the “generalized min-max” (GMM) kernel as a measure of data similarity, to effectively capture data nonlinearity. The GMM kernel can be linearized via the generalized consistent weighted sampling (GCWS). Our experimental study demonstrates that usually GCWS does not need too many samples in order to achieve good accuracies. In particular, GCWS typically requires substantially fewer samples to reach the same accuracy as the random Fourier feature (RFF) method. This is practically important, because the training (and testing) cost is largely determined by the number of nonzeros (which is the same as the number of samples in RFF or GCWS) per data vector of the dataset. We expect that GMM and GCWS will be adopted in practice. Lastly, we should also mention that GCWS can be naturally applied in the context of sublinear time near neighbor search, due to the discrete nature of the samples.

## References

- [1] R. H. Affandi, E. Fox, and B. Taskar. Approximate inference in continuous determinantal processes. In *NIPS*, pages 1430–1438. 2013.
- [2] L. Bottou. <http://leon.bottou.org/projects/sgd>.
- [3] L. Bottou, O. Chapelle, D. DeCoste, and J. Weston, editors. *Large-Scale Kernel Machines*. The MIT Press, Cambridge, MA, 2007.
- [4] K. P. Chwialkowski, A. Ramdas, D. Sejdinovic, and A. Gretton. Fast two-sample testing with analytic representations of probability measures. In *NIPS*, pages 1981–1989. 2015.
- [5] B. Dai, B. Xie, N. He, Y. Liang, A. Raj, M.-F. F. Balcan, and L. Song. Scalable kernel methods via doubly stochastic gradients. In *NIPS*, pages 3041–3049. 2014.
- [6] R.-E. Fan, K.-W. Chang, C.-J. Hsieh, X.-R. Wang, and C.-J. Lin. Liblinear: A library for large linear classification. *Journal of Machine Learning Research*, 9:1871–1874, 2008.
- [7] T. J. Hastie, R. Tibshirani, and J. H. Friedman. *The Elements of Statistical Learning: Data Mining, Inference, and Prediction*. Springer, New York, NY, 2001.
- [8] J. M. Hernández-Lobato, M. W. Hoffman, and Z. Ghahramani. Predictive entropy search for efficient global optimization of black-box functions. In *NIPS*, pages 918–926. 2014.
- [9] C.-J. Hsieh, S. Si, and I. S. Dhillon. Fast prediction for large-scale kernel machines. In *NIPS*, pages 3689–3697. 2014.
- [10] S. Ioffe. Improved consistent sampling, weighted minhash and L1 sketching. In *ICDM*, pages 246–255, Sydney, AU, 2010.

- [11] H. Larochelle, D. Erhan, A. C. Courville, J. Bergstra, and Y. Bengio. An empirical evaluation of deep architectures on problems with many factors of variation. In *ICML*, pages 473–480, Corvallis, Oregon, 2007.
- [12] P. Li. Abc-boost: Adaptive base class boost for multi-class classification. In *ICML*, pages 625–632, Montreal, Canada, 2009.
- [13] P. Li. Robust logitboost and adaptive base class (abc) logitboost. In *UAI*, 2010.
- [14] P. Li. 0-bit consistent weighted sampling. In *KDD*, Sydney, Australia, 2015.
- [15] P. Li. Nystrom method for approximating the gmm kernel. Technical report, arXiv:1605.05721, 2016.
- [16] P. Li, T. J. Hastie, and K. W. Church. Improving random projections using marginal information. In *COLT*, pages 635–649, Pittsburgh, PA, 2006.
- [17] P. Li, G. Samorodnitsky, and J. Hopcroft. Sign stable projections, sign cauchy projections and chi-square kernels. Technical report, arXiv:1308.1009, 2013.
- [18] P. Li, A. Shrivastava, J. Moore, and A. C. König. Hashing algorithms for large-scale learning. In *NIPS*, Granada, Spain, 2011.
- [19] P. Li and C.-H. Zhang. Theory of the gmm kernel. Technical report, arXiv:1608.00550, 2016.
- [20] M. Manasse, F. McSherry, and K. Talwar. Consistent weighted sampling. Technical Report MSR-TR-2010-73, Microsoft Research, 2010.
- [21] M. Raginsky and S. Lazebnik. Locality-sensitive binary codes from shift-invariant kernels. In *NIPS*, pages 1509–1517. 2009.
- [22] A. Rahimi and B. Recht. Random features for large-scale kernel machines. In *NIPS*, 2007.
- [23] E. Richard, G. A. Goetz, and E. J. Chichilnisky. Recognizing retinal ganglion cells in the dark. In *NIPS*, pages 2476–2484. 2015.
- [24] W. Rudin. *Fourier Analysis on Groups*. John Wiley & Sons, New York, NY, 1990.
- [25] A. Shah and Z. Ghahramani. Parallel predictive entropy search for batch global optimization of expensive objective functions. In *NIPS*, pages 3330–3338. 2015.
- [26] D. J. Sutherland and J. Schneider. On the error of random fourier features. In *UAI*, Amsterdam, The Netherlands, 2015.
- [27] T. Yang, Y.-f. Li, M. Mahdavi, R. Jin, and Z.-H. Zhou. Nyström method vs random fourier features: A theoretical and empirical comparison. In *NIPS*, pages 476–484. 2012.
- [28] I. E.-H. Yen, T.-W. Lin, S.-D. Lin, P. K. Ravikumar, and I. S. Dhillon. Sparse random feature algorithm as coordinate descent in hilbert space. In *NIPS*, pages 2456–2464. 2014.